Received: October 6, 2019. Revised: October 30, 2019.

International Journal of
Intelligent Engineering & Systems

http://www.inass.org/

A New Method to Enhance Fingerprint Image Reconstruction Using Deep Boltzmann Machine

Nouf Saeed Alotaibi[1]*

[1] *Computer Science Department, College of Science, Shaqra University, Saudi Arabia*
* Corresponding author's Email: n.saeed@su.edu.sa

Abstract: A new algorithm for increasing fingerprint with large noise is enhanced in this paper. The fingerprint image is first pre-improved depending on Gabor filters, and local adaptive thresholds are used to achieve a binary fingerprint. In order to reconstruct these regions, which have incorrectly improved in the first stage, the classification deep Boltzmann machines (DBMs) with a range pattern before are used. The proposed technique completely enhances each other by a traditional technique of improvement relying upon Gabor filtering and deep learning. The FVC 2004, Biometrika, Italdata, Crossmatch, and Swipe databases are conducted by different techniques. Experiments indicate that in contrast with other techniques, the suggested technique achieves stronger outcomes and enhances fingerprint performance. Experimental findings indicate that the use of the proposed technique allows the extremely accurate fingerprint image to be reconstructed. The average performance of the proposed method is 91.31, which is better than the average performance of another method. When there exist 18,000 features, the running time of UniNap1, ATVS, Dermalog, and CAoS are 68, 74, 59, 87 s respectively, while the running time of the proposed method is 45s.The proposed technique is superior for removing noise than other techniques, in particular for improving fingerprints of poor performance.

Keywords: Fingerprint improvement, Gabor filter, Image reconstruction, Deep Boltzmann machine, Classification.

1. Introduction

Biometric authentication means the verification of individuals based on their physiological and behavioral properties. Biometric technology is now widely used for different purposes of personal authentication in many applications [1, 2]. The fingerprint recognition technology is one of the best known biometric technologies because of its consistency and its uniqueness in life [3, 4]. Many automatic fingerprint identification systems (AFISs) are minutiae matching based [5, 6]. Exactly the quality of the fingerprint image is largely a factor in the accuracy and safety of minutiae extraction [7, 8, 9]. Various methods of improvement described in the literature [10, 11, 12] can improve the quality of fingerprints. Hong et al. [7] implemented a Gabor filtering method to improve fingerprint, which is the most popular method [13]. The classical Gabor filter is parameter sensitive and depends heavily on the fingerprint quality of the input [14, 15]. To resolve this constraint, many researchers have proposed improved Gabor algorithms [9, 10] but each has a variety of defects, respectively. Sutthiwichaiporn et al. suggested adaptive enhanced spectral filtering (ABSF) for gradual fingerprint improvement [14]. A Gaussian matched filter from high-quality areas is applied, and then the excellent spectrum of improved ridges is iteratively distributed in lower-quality areas. The algorithm suggested is largely based on the patch's priority. In [14] the noise was eliminated and noise peak was estimated using a relatively random difficult threshold, which then achieves a ridge signal and priority in the patch quality. The spectrum allocation of the ridge is distinct, however, in various patches and in certain instances it will lead to mistakes. The Deep Belief Networks (DBNs) [16, 17] offered a useful means to construct deep networks that open up research in deep learning. In the last 10 years, deep learning theories and apps have been researched extensively [18-20]. In recent years some key technologies for fingerprint identification based on deep learning have been devoted to the outstanding performance of deep learning in the field of image processing [21]. The DBM is an undirected graphic model centered on a limited Boltzmann machine (RBM). DBM utilizes RBMs first to layer-by-layer pre-train network weights and then employs the correct technique to adjust weights [18]. The DBM demonstrates excellent classification capabilities as well as effective image reconstruction abilities, particularly appropriate for binary image reconstruction.

We suggest a new fingerprint improvement technique that mixes frequency-domain filtering with classified DBM reconstruction to solve the failures of the traditional fingerprint improvement process driven by the latest achievement of DBM image reconstruction.

The new features of the proposed method perform Gabor filtering to pre-enhance fingerprint in the spatial domain. Properly tuned Gabor filters to the corresponding local orientation and ridge frequency, the noise can be removed, preserve the genuine ridge and valley structures, and provide information contained in a particular orientation in the fingerprint. We can note that the proposed method can improve regions with strong noise. we used classification DBMs model for each class patches to capture the more reliable ridge pattern prior, significantly enhancing the performance of fingerprint reconstruction, instead of using a DBM model for all patches. In addition, instead of detecting similar patches, we detect the patches with high quality in each class as a corresponding classification DBMs training set to construct a reliable training set. In our experiment, the pre-enhanced binary fingerprint patches with low quality are reconstructed according to their own ridge pattern constraint, so it is easy to make sure that the ridges can be enhanced reliably. Our method is compared to other methods and can report that the proposed method is better for enhancing fingerprint images. The test results of the proposed and other methods show that the fingerprint with low quality can be accurately improved by using the proposed method.

The rest of the paper is arranged accordingly. Section 2 presents the related works in a short overview. The original fingerprint will be updated and binarization in Section 3 to obtain the pre-enhanced binary fingerprint. Paragraph 4 focuses on reconstructing fingerprints, describing DBM classifications and restoring fingerprints in depth. Section 5 reports and analyzes experimental outcomes. Finally, some conclusions are drawn in Section 6.

2. Related works

2.1 The patch orientation estimation of fingerprint

In fingerprint recognition systems, there are two common directions have been identified for detecting the fingerprint: 1) the active liveness features of fingerprint detectors, for instance, by examining pulse, perspiration patterns and blood pressure; 2) Passive pattern analyzer for fabricating materials, for instance, the lack of details of spoofed fingerprints according to the real ones, fingerprint pattern differences. The last type problem is the scope of our proposed method.

The quality of fingerprint images can be corrupted by various kinds of a noise. It is still a challenge for scientists to remove the noise from fingerprint images. Removing this noise from a fingerprint image must estimate their original image while preserving the relevant features edges, textures, and details. The traditional Gabor filter is sensitive to parameters and heavily relies on the quality of the input fingerprint. In the traditional method, unprocessed gray-scale fingerprint images usually contain unwanted artifacts caused by a skin condition and sensor noise. Enhancement and separation of fingerprints from the background denoted binarization is frequently employed as a pre-processing step in the fingerprint recognition systems to reduce the unwanted artifacts. In order to obtain the binary fingerprint image, the gray fingerprint is converted to a binary one by a simple local adaptive threshold algorithm. In this paper, the fingerprint image is divided into non-overlapping patches, and the local adaptive threshold can be obtained by the gray intensity mean of the patch. In order to overcome the shortcomings of the traditional fingerprint enhancement methods, motivated by the recent success of the DBM in image reconstruction, we propose a novel fingerprint enhancement method that combines a frequency-domain filtering and classification DBMs reconstruction.

The objective of the patch orientation estimate is to identify the local composition and orientation of the ridges within the image of the fingerprint. The easiest and most regular way of assessing the orientation of the patch ridge is to determine the local gradients. Kass and Witkin carried out the pioneering research of the gradients-based technique in [22], in which the vectors of the patch gradient compute the local orientation. The idea of doubling the orientation angles was introduced, and the local window was averaged with a separate x- and y-component. Bazen et al. [23] used the average technique of square gradients for local direction calculations. This technique has different anti-noise capabilities when the patch size increases and is weak when the patch is small and when the patch is large, it is enhanced. There are various ways of seeing the modulus of the vector gradient as normal in the gradient techniques. In [23] the gradient angle is not only doubled but also the length of the gradient vector is squared. The gradient is tightly linked to the gradient module. The stronger gradients have greater votes in the calculation of local orientation than the weaker ones. On the contrary, some scientists [25] believed that we are involved exclusively in the orientation, and the modulus only shows a contrast to the image, so we must normalize the modulus. In [26], the researchers evaluate the impact on estimate efficiency of the gradient normalization modulus and demonstrate the benefit and the disadvantage of gradient modulation normalization. The fingerprint orientation domain is calculated using standard and un-normal point gradient vectors for evaluating and analysing the influence of the orientation estimates using the two distinct techniques listed above [27]. The analysis shows that efficient point gradient vectors (which are situated on the edges between ridges and valleys) frequently have beneficial results, while inactive point gradient vectors (often situated within ridges or valleys with small-module or at the edges of a sudden noise with distinctly huge modulus) often have side effects. Based on historical studies [24], Bian et al. [28] suggested predicting the local orientation a weighted LPA algorithm based on a likeness of point gradient orientation. The efficacy of the vector was evaluated based on the resemblance of the point gradient orientations. Let a point gradient vector be oriented in the local region is $\theta_j (j = 1, \ldots, P^2)$, the patch size is $P \times P$. Then, the similarity measure S_j is calculated by

$$S_j = \frac{1}{P^2} \sum_{m=1}^{P^2} \frac{\cos(\theta_j - \theta_m) + 1}{2} \tag{1}$$

Let us define the gradient vector set of the patch as, $V_j (j = 1, \ldots, P^2)$, it can show as the following

$$V_j = \begin{bmatrix} G_{jx}(x,y) \\ G_{jy}(x,y) \end{bmatrix} \tag{2}$$

Where $[G_{jx}(x,y), G_{jy}(x,y)]^T$ is the gradient vector.

According to the literature, we can find the equation [28]:

$$V_s = \sum_{j=1}^{P \times P} R_j^2 \, V_j V_j^T = \begin{bmatrix} G_{xx} & G_{xy} \\ G_{xy} & G_{yy} \end{bmatrix} \tag{3}$$

Where

$$G_{xx} = \sum_{j=1}^{P \times P} R_j^2 \, G_{jx}^2, G_{yy} = \sum_{j=1}^{P \times P} R_j^2 \, G_{jy}^2,$$
$$G_{xy} = \sum_{j=1}^{P \times P} R_j^2 \, G_{jx} \, G_{jy}$$

Where R_j is the similarity. The similarity shows the differentiation between the orientation of arbitrary points and the others in same block. It indicates whether this point orientation is important while computing the local optimum orientation.

According to Eq. (3) the eigen values of V_s can be described as the following:

$$\tau_1 = \frac{(G_{xx} + G_{yy}) + \sqrt{(G_{xx} + G_{yy})^2 + 4G_{xy}^2}}{2},$$

$$\tau_2 = \frac{(G_{xx} + G_{yy}) - \sqrt{(G_{xx} + G_{yy})^2 + 4G_{xy}^2}}{2} \tag{4}$$

We can calculate the eigenvector u_1 which corresponds to the maximum eigenvalue τ_1 as the following:

$$u_i = \begin{bmatrix} (G_{xx} + G_{yy}) + \sqrt{(G_{xx} + G_{yy})^2} + 4G_{xy}^2 \\ 2G_{xy} \end{bmatrix} \tag{5}$$

The estimated value of the dominant gradient orient ation can then be calculated in the local region by

$$\varphi = tan^{-1} \left(\frac{2G_{xy}}{(G_{xx} + G_{yy}) + \sqrt{(G_{xx} + G_{yy})^2} + 4G_{xy}^2} \right) \tag{6}$$

The ridge orientation can be calculated by

$$\theta = \varphi + \frac{1}{2}\pi \tag{7}$$

2.2 Local adaptive threshold fingerprint binarization

Usually unwanted artifacts from a skin situations and noise from sensor images comprise unprocessed fingerprint gray-scale. The gray fingerprint is transformed to binary with a local adaptive threshold algorithm in order to get the binary fingerprint image. In this case, the fingerprint image Im is divided into un-overlapping patches of size $P \times P$, while the gray

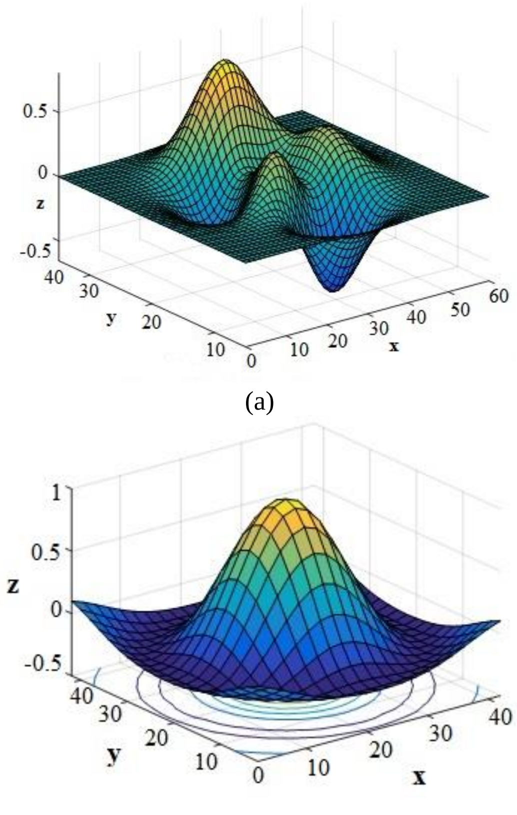

(a)

(b)

Figure.1 shows different examples for evenly symmetrical Gabor filter in the spatial domain

intensity mean of the patch can achieve the local adaptive threshold.

$$T_{avg} = \frac{1}{P \times P} \sum_{m=1}^{W} \sum_{n=1}^{W} Im(m,n) \quad (8)$$

Where $Im(m,n)$ is the fingerprint image which, divided into un-overlapping patches of size $P \times P$.

Then, a new value (1 or 0) is set to the following thresholds for each pixel in the local patch as follows:

$$Im(m,n) = \begin{cases} 0\,, & if\ Im(m,n) \le T_{avg} \\ 255\,, & otherwise \end{cases} \quad (9)$$

3. Fingerprint pre-enhancement and binarization

Gabor function has been identified in particular for texture analysis as a very powerful tool for computer vision and image processing. Gabor filters have both frequency selective and orientation selective characteristics and are jointly resolution in the spatial field as well as in the frequency field [29]. In a local and constant orientation in the fingerprint image, the sinusoidal waves of ridges and valleys slowly vary. Thus, an unwanted noise can be effectively removed, and the true ridge and valley structures can be preserved by a filter that is tuned to their frequency and orientation. The Gabor filter is evenly symmetrical in the general form:

$$G(x,y;\theta,f) = \exp\left(\frac{-1}{2}\left(\frac{x_\theta^2}{\delta_x^2} + \frac{y_\theta^2}{\delta_y^2}\right)\right)\cos(2\pi f x_\theta) \quad (10)$$

$$x_\theta = x cos\theta + y sin\theta \quad (11)$$

$$y_\theta = -x sin\theta + y cos\theta \quad (12)$$

The frequency of a wave of the sinusoidal plane and δ_x *and* δ_y are Gaussian envelope constants on the x and y axes, respectively. Fig. 1 shows the spatial features of Gabor filters.

In this paper, we used the Gabor filter to pre-improve the fingerprint in the spatial domain. See literature [4] for information on this operation. They believed in their algorithm, which fingerprints everyone has local parallel ridges and valleys, and a straightforward local orientation and frequency. There are some perfect sinusoidal-shaped planes connected with some noises on the parallel ridges and valleys. We are able to remove noise, maintain genuine ridge and the valley structures and provide data in a specific fingerprint orientation and properly adjusted Gabor filters at the respective local orientation and ridge frequency. The earlier sinusoidal plane wave thought to be [4] is wrong, moreover, because, in reality, in several fingerprints or in certain places (particularly in high noise areas), the orthogonal signal is not an optimal digital sinusoidal plane wave. The improvements therefore allow a great deal to be wanted in these areas. Two instances of the pre-improvement of the fingerprint are illustrated in Fig. 2. FVC2004 DB3_A 37_6 and 39_1 have been used for sample fingerprints. From the image. 2(b), it can be seen that the Gabor improvement method enhances transparency of the original fingerprint image ridge and valley constructions in areas with a low noise, but in areas of high noise it has achieved little to improve it. The pre-improved fingerprint must be transformed to binary images in the attempt to use classified DBMs to reconstruct the poor performance fingerprint region. You can access a binary fingerprint image using the technique illustrated in section 2.2. A fingerprint binarization instance is provided in 2(c). The results suggest that the local adaptive threshold is easy to calculate but efficient in the binarization of the fingerprint.

Received: October 6, 2019. Revised: October 30, 2019.

4. Fingerprint reconstruction based on Classification DBMs

4.1 Classification DBMs model construction

The fingerprint has a constant and reliable ridge pattern, as opposed to standard image reconstruction. To achieve a significant reconstruction of fingerprints, an efficient preliminary or limitation is an important matter for a reconstruction algorithm. By using the pattern of the ridge before fingerprints, we classify fingerprint patches by its own pattern of the ridge orientation. Rather than learning merely to use a DBM model across all parts, we discover DBM classifications for the patches per class to capture the more reliable ridge pattern prior, which enhance the efficiency of fingerprint reconstruction considerably. The patch with high quality is chosen for each class in the respective DBM classification training set in order to generate a credible learning sample set instead of choosing common patches. The Boltzmann Deep Machines is a type of RBM-based deep learning model proposed in [18]. The DBM is a graph model that is undirected, has numerous hidden layers but only links to neighbouring layers. For instance, we show the model structure of a DBM model in Fig.3, with two hidden layers.

It expresses the energy function as:

$$G(x,y;\theta,f) = -\sum_{i=1}^{I}\sum_{j=1}^{J} V_i P_{ij}^1 h_j^1 - \sum_{j=1}^{J}\sum_{l=1}^{L} h_j^1 P_{jl}^2 h_l^2 - \sum_{j=1}^{J} b_j h_j^1 - \sum_{l=1}^{L} a_l h_l^2 - \sum_{i=1}^{I} c_i V_i \quad (13)$$

Where $a = \{a_l\}_{l=1}^{L}$, $b = \{b_j\}_{j=1}^{J}$ and $c = \{c_i\}_{i=1}^{I}$.

The bias vectors of visible layer V are $a, b,$ and c. h^1 and h^2 are two hidden layers. P^1 and P^2 are visible-to-hidden and hidden-to-hidden symmetric interaction terms, respectively. The conditions probabilities of the DBM can be determined by:

$$p\left(h_j^1 = 1|V, h^2\right) = \tau\left(\sum_i P_{ij}^1 v_i + \sum_l P_{jl}^2 h_l^2 + b_j\right) \quad (14)$$

$$p\left(h_l^2 = 1|h^1\right) = \tau\left(\sum_j P_{jl}^2 h_j^1 + a_l\right) \quad (15)$$

$$p\left(v_i = 1|h^1\right) = \tau\left(\sum_j P_{ij}^1 h_j^1 + c_i\right) \quad (16)$$

Where $\tau(x) = \frac{1}{(1+\exp(-x))}$.

The DBM utilizes RBMs to pre-train network weights layer by layer. Salakhutdinov and others [18] use the greedy layer-by-layer of pre-training algorithms to simultaneously train various RBMs, as can be seen in Fig. 4. Then, these RBM's are combined and the comprehensive description can be discovered in literature [18]. Initial DBM scores are acquired. Following the selective pre-training method, the DBM needs to refine the weights of the network and provide information. In algorithm 1. $\alpha_P, \alpha_v,$ and α_b are the leaning rates of the weights, the bias terms of the visible layer and the bias terms of the hidden layer, respectively. In this paper, we categorize training fingerprint patches into 8 communities using their own ridge orientation pattern to achieve an efficient previous or limit and we learn 8 ranking DBMs for each category each patch, respectively.

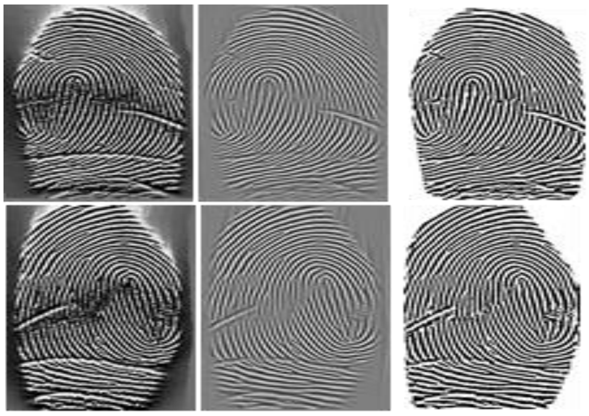

(a) (b) (c)

Figure.2 Fingerprint pre-enhancement and binarization: (a) the original input fingerprint image, (b) the corresponding enhancement fingerprints based on Gabor filtering, and (c) the binary fingerprint

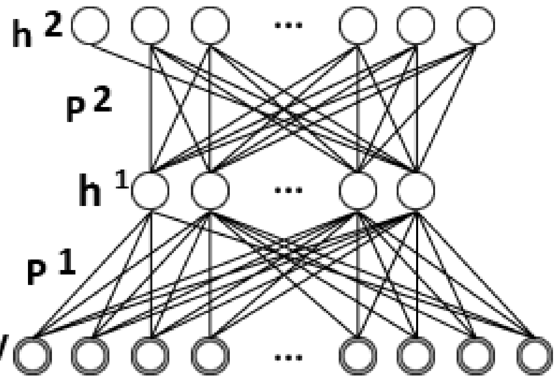

Figure.3 The model structure with the two hidden layers of the deep Boltzmann machine

Received: October 6, 2019. Revised: October 30, 2019.

Table 1. Exact modification of the weights of a two hidden layer DBM for fingerprint patch

Algorithm 1 exact modification of the weights of a two hidden layer DBM for fingerprint patch
1. **Input**: a train set of N binary data vectors $\{V\}_{n=1}^{N}$, and the number of Gibbs sampling K.
2. Samples start E: { v^0 , $h^{1\,0}$, $h^{2\,0}$ },…, {v^E,$h^{E\,0}$,$h^{2\,E}$}.
3. Get the weights {c, P^1, b, P^2, a} that trained in greedy pre-training step.
4. For q=1 to Q (where Q is the number of iterations) do
5. //Variation Inference:
6. For every training sample $v^n \rightarrow$ n=1 to N do
7. Set vectors $h^1 = \tau(v^n\left(2P^1\right) + b)$, $h^2 = \tau(h^1P^2 + a)$, operate average field to update h^1 and h^2 until convergence: $h^1 = \tau(v^n P^1 + h^2 (P^2)^T + b)$, $h^2 = \tau(h^1P^2 + a)$
8. Set $\beta_{h^1}^{n} = h^1$, $\beta_{h^2}^{n} = h^2$
9. End for
10. //Stochastic Approximation:
11. For r=1 to R do
12. For every fresh sample v^m, m=1 to M do
13. Sample { $v^{m\,k}$, $h^{1m\,k}$, $h^{2m\,k}$ } given { $v^{m\,k-1}$, $h^{1m\,k-1}$, $h^{2m\,k-1}$ }as follows Eqs. (14)-(16).
14. End for
15. End for
16. //Parameters Update
17. $P^1 = P^1 + \alpha_w((\sum_{n=1}^{N} v^n\ (\beta_{h^1}^{n})^T)/N - (\sum_{m=1}^{M} v^{m\,K}\ (h^{1m\,k})^T)/M)$
18. $P^2 = P^2 + \alpha_w((\sum_{n=1}^{N} \beta_{h^1}^{n}\ (\beta_{h^2}^{n})^T)/N - (\sum_{m=1}^{M} h^{1m\,K}\ (h^{2m\,k})^T)/M)$
19. $c = c + \alpha_v((\sum_{n=1}^{N} v^n)/N - (\sum_{m=1}^{M} v^{m\,K})/M)$
20. $b = b + \alpha_b((\sum_{n=1}^{N} \beta_{h^1}^{n})/N - (\sum_{m=1}^{M} h^{1m\,K})/M)$
21. $a = a + \alpha_b((\sum_{n=1}^{N} \beta_{h^2}^{n})/N - (\sum_{m=1}^{M} h^{2m\,K})/M)$
22. Decrease α_b, α_v, α_w.
23. End for

To do training and testing samples of fingerprints in the dataset, we have tried various values of specific parameters: $\alpha_w, \alpha_v,$ and α_b respectively on our experiments. Appropriate values for these parameters are chosen.

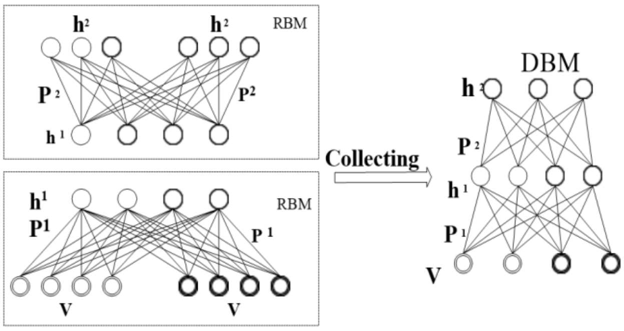

Figure. 4 Avaricious DBM pre-training with two hidden layers

4.2 Selection of the reconstruction patches

The reconstruction relying on DBM must be noted for its increased time complexity over moment. Ideally, only the fingerprint patches with noise must be reconstructed, and the technique suggested improves effectiveness. It is essential to assess the performance of these reconstruction patches in an attempt to attain this objective and then assess if they need to be reconstructed. In this phase, we simply ensure that the assessments of the patches to be reconstructed are reliable and that the low-quality patches are reconstructed in a way. Although the accuracy of the assessment findings cannot be guaranteed entirely, it guarantees that the evaluation results of the parts to be reconstructed are reliable.

In order to calculate the quality of fingerprint patch, we divide a fingerprint into overlapping A×B patches, and the quality type of a patch (i, j) is defined as a fingerprint patch, $H_b(i,j)$ $(i = 1,2,\ldots,A; j = 1,2,\ldots,B)$. The patch quality can be computed by the coherence of point orientations [24, 28], which can be defined by Eq. (4).

$$Coh = (\tau_1 - \tau_2)/((\tau_1 + \tau_2)) \tag{17}$$

The patch performance sort can be assessed according to coherence.

$$H_b(i,j) = \begin{cases} 1, & if\ Coh \in [0.8,\ 1] \\ 2, & otherwise \end{cases} \tag{18}$$

We only have to reconstruct low-quality. Fig.5 (b) and (d) demonstrate two instances of a coherent performance assessment and classification, the corresponding original fingerprint see Fig.2. It also can guarantee accuracy of the reconstruction patches and almost definitely not misunderstand the low-quality patch, which must be reconstructed as a high-quality patch. The suggested technique shows that the time cost of the reconstruction dependent on DBM may be reduced efficiently.

Received: October 6, 2019. Revised: October 30, 2019.

(a) (b) (c) (d)

Figure. 5 The quality assessment and classification: (a) the original fingerprint, (b) results of classification by the coherence, and (c) results of classification by the variance, where the red, green, blue and black represent high, medium, low and bad quality types respectively

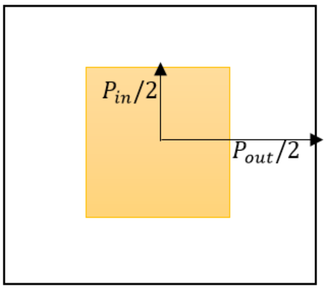

Figure. 6 Template for the composite window

4.3 Reconstruction of the fingerprint

The fingerprint pre-enhancement is divided into intersecting patches in spatial domain. Section 4.2 selects the patches that must be reconstructed. The patches are reconstructed by means of classification DBMs depending on a composite window. We introduce the idea of composite window (CW) in order to take full benefit from high quality ridge information to reconstruct this ridge. As illustrated in Fig. 6, the composite window comprises in this method of an inner and outer window and both have the same central point, and $P_{in} \leq P_{out}$.

When reconstructing a fingerprint patch on the specified entry patch, it is first calculated the orientation of this patch using the technique outlined in section 2.1, and then this patch is immediately categorized according to its orientation to the appropriate class. The input patch is finally reconstructed with the appropriate DBM classification. The reconstruction patch performance is also more assured.

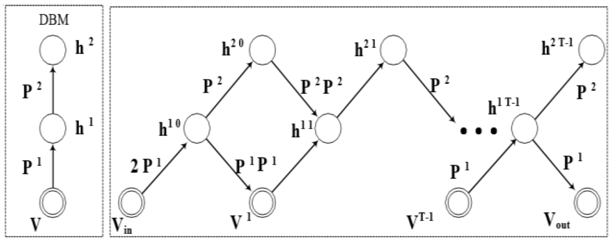

Figure. 7 Shows the diagram of reconstruction of the fingerprint patch dependent on classification DBMs

(a) (b) (c) (d) (e) (f)

Figure. 8 Instances of the reconstruction of fingerprint patches using DBMs: (a), (c) and (e) reconstructed patches with large noise and (b), (d) and (f) identical reconstruction patches

Table 2. Reconstruction fingerprint patch depending on DBM

Algorithm 2 Reconstruction fingerprint patch depending on DBM

1. Input: The patch to be reconstructed with large noise V_{in}.
2. Initialize $h^{1\,0} = \tau(V_{in}(2P^1) + b)$, and $h^{2\,0} = \tau(h^{1\,0}P^2 + a)$
3. For z=1 to Z (the total number of iterations) do
4. //Mean Field Updates
   $v^z = \tau(h^{1\,z-1}P^1 + c)$
   $h^{1\,z} = \tau(v^z P^1 + h^{2\,z-1}P^2 + b)$
   $h^{2\,z} = \tau(h^{1\,z}P^2 + a)$
5. End for
6. Output: $V_{out} = V^T$

The patch can readily be reconstructed by using the mean field technique once the Classification DBMs are constructed. Fig. 7 illustrates the entire patch reconstructing process from the input patch, in V_{in} is the input patch, out V_{out} is the reconstructed patch, we provide the details in algorithm 2. A few instances of the restoration of fingerprint patches using classification DBMs are presented in Fig. 8. We can say that the technique suggested can correctly and reliably reconstruct fingerprint patches.

We must incorporate the ridge information with high quality as much as possible into the patch with low quality to achieve the best DBM reconstruction. The patches are first reconstructed surrounded by the highest quality. The patches will therefore be reconstructed to the preference of the neighbourhood. The neighbourhood priority N_{pri} is defined as follows:

$$N_{pri} = \begin{cases} 1, & if\ Num_{Nei} \geq 6 \\ 2, & if\ 5 \geq Num_{Nei} \geq 4 \\ 3, & otherwise \end{cases} \quad (19)$$

Where Num_{Nei} is number of improved patches in eight neighbourhood. The detailed suggested method fingerprint can be seen in Fig. 9.

Received: October 6, 2019. Revised: October 30, 2019.

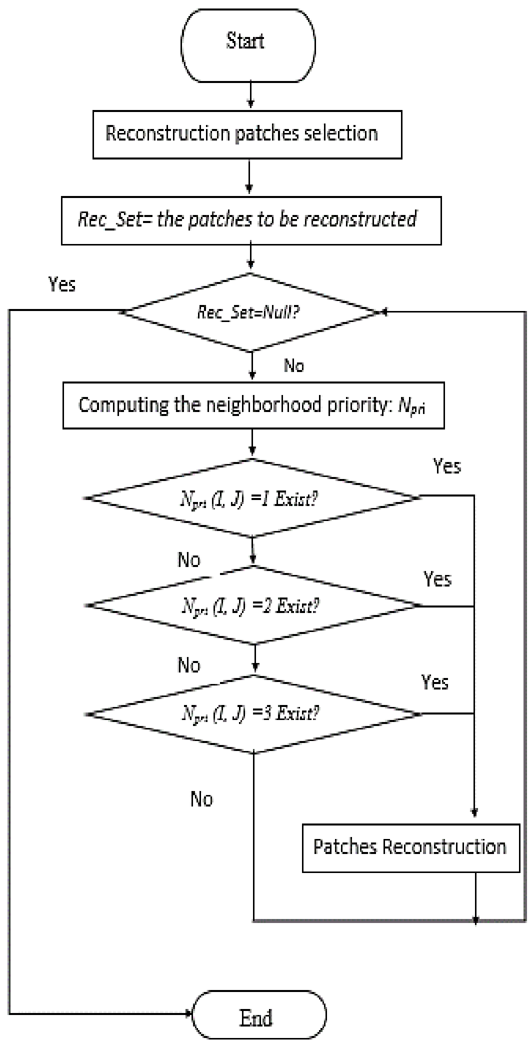

Figure.9 Flowchart of the fingerprint reconstruction depend on classification DBMs

5. Experimental results

The public fingerprint database FVC 2004 is used to analyse and evaluate more fully the efficiency of the proposed method. The fingerprints are improved with soft Veri-Finger Algorithm Demo to construct the training set for DBMs for learning classification and then divided into patches to comprise the training patch collection. The inner patch of composite window size is composed of 16 × 16 pixels, the relevant external patch size is composed of 32×32 pixels, and the slide window is 10 pixels. The training patches are divided into 8 groups according to their own ridge of ridge orientation. The 8 classification DBMs are trained depending on the appropriate classification training set. Experimental findings indicate that the use of the proposed technique allows the extremely accurate fingerprint image to be reconstructed. Fig. 2 provides two instances of pre-improvement and binarization of fingerprint. Fig. 2

Figure.10 Fingerprint reconstruction using classification DBMs based on fingerprint patch quality evaluation: (a) and (c) pre-enhancement and binarization fingerprint, and (b) and (d) fingerprint reconstruction based on classification DBMs

provides two instances of pre-improvement and binarization of fingerprint. We can see that in areas with low noise fingerprints are well improved, but in areas with high noise, labeled in red circular boxes in the fig. 10 (a) and (c). We are now using classification DBMs to reproduce these regions with large noise. Fig. 10 demonstrates a DBM-classified fingerprint. As mentioned earlier in section 4.2, the patches that need to be reconstructed are evaluated, as indicated in the fig. 5(b) and (d), respectively. In order to enhance the efficiency of the proposed method. The respective results are shown in Fig.10 (b) and (d) by using Classification DBMs. We can find that the approach suggested can essentially guarantee the reliability of patch examinations of high quality as well as certainly not misunderstand the patch of low quality as a high-quality patch. It guarantees that all large noise patches can be reconstructed. In the meantime, the patches with large noise are accurately reconstructed with classification DBMs with a ridge pattern.

We have conceived a sample experiment to evaluate the efficiency of the suggested technique using the filtering technique combining with the spectrum diffusion offered in [30] and VeriFinger Software, where the suggested technique is contrasted with the ABSF [14]. In Fig.11 shows the two group tests, FVC2004 DB3_A 38_8 and 86_1 are used to sample fingerprint images. In Fig. 11 shows that the ABSF-enhanced fingerprint and VeriFinger-enhanced fingerprint regions with low noise have been well enhanced, but the high-noise regions are not satisfactorily enhanced. In contrast, the proposed technique is superior for removing noise than other techniques, in particular for improving fingerprints of poor performance. Our expertise reconstructs pre-enhanced, low-quality binary fingerprint patterns according to their own ridge pattern constraints and makes it simple to ensure that the ridges can be

Received: October 6, 2019. Revised: October 30, 2019.

Table 3. Detection accuracy measured with Biometrika, Italdata, Crossmatch, and Swipe datasets. Dermalog and UniNap1 results are from [31]

method / datasets	proposed	UniNap1 [31]	ATVS [32]	Dermalog [31]	CAoS [32]
Biometrika	99.46	95.30	82.49	98.30	88.42
Italdata	98.81	96.50	91.60	99.20	90.34
Crossmatch	69.96	68.80	39.74	44.53	41.79
Swipe	97.01	85.93	58.84	96.47	60.58
Average	**91.31**	86.58	68.17	84.63	70.28

reliably improved. We can only hope for our method of doing this. The experiment outcomes shown in the figure are also described in Fig. 10. Therefore, to overcome the clash between enhanced ridge and removing noise the suggested technique is more effective.

In the traditional method, unprocessed grayscale fingerprint images usually contain unwanted artifacts caused by skin condition and sensor noise. Enhancement and separation of fingerprints from the background denoted binarization is frequently employed as a preprocessing step in the fingerprint recognition systems to reduce the unwanted artifacts. In order to obtain the binary fingerprint image, the gray fingerprint is converted to binary one by a simple local adaptive threshold algorithm. In this paper, the fingerprint image divided into non-overlapping patches, and the local adaptive threshold can be obtained by the gray intensity mean of patch. In order to overcome the shortcomings of the traditional fingerprint enhancement methods, motivated by the recent success of the DBM in image reconstruction, we propose a novel fingerprint enhancement method that combines frequency-domain filtering and classification DBMs reconstruction.

Figure.11 The contrast experiment outcomes of fingerprint improvement: (a) original fingerprint, (b) ABSF [14], (c) Bian et al. [30], (d) VeriFinger Software, (e) pre- improvement and binarization based on proposed technique, and (f) reconstructed fingerprint depend on DBMs with ridge pattern prior

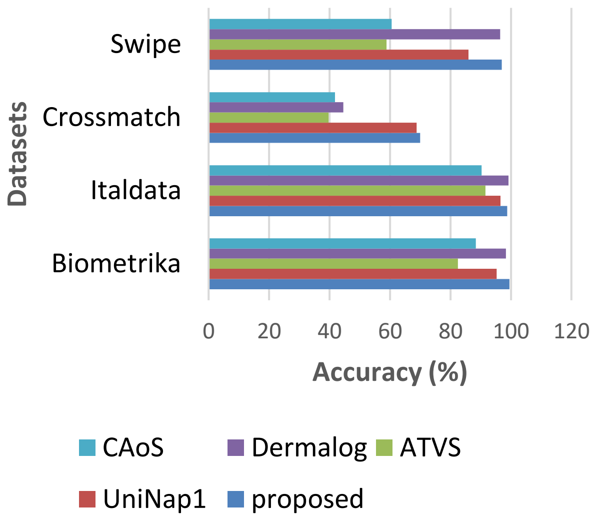

Figure.11 Detection accuracy evaluated with Biometrika, Italdata, Crossmatch, and Swipe datasets

Table 3 demonstrates the detection accuracy evaluated with Biometrika, Italdata, Crossmatch, and Swipe datasets. The average classification error (ACE) is used to evaluate the performance of the UniNap1 [31], ATVS [32], Dermalog [31], CAoS [32], and proposed methods. From Table 3, we note that the proposed method is better than other methods. The average performance of the proposed method is 91.31, which is superior to the average performance of another methods.

Fig. 11 demonstrates the detection accuracy evaluated with Biometrika, Italdata, Crossmatch, and Swipe datasets. To evaluate the time complexity of the proposed method, various number of image features used to measure the computation time of the proposed method. The execution time of the proposed method based on 128 features is 39 seconds. In the proposed method, the running time for 18,000 features is increased to 45 s which is slightly high which is still the future direction to reduce the time computation. While, the running time of UniNap1 [31], ATVS [32], Dermalog [31], CAoS [32] are 68, 74, 59, 87 s, respectively. It is clear that the running time of the proposed method is faster than other methods.

6. Conclusion

In this paper, we try to investigate the new fingerprint improvement technique and suggest a robust, predominantly grid pattern-based fingerprint improvement technique based on DBMs classification. The fingerprint is pre-improved by Gabor filtering as well as the binary fingerprint is achieved by local adaptive threshold binarization. The classification DBMs with the ridges pattern are learned prior to reconstructing those regions with large noise at fingerprint pre-enhancement. The ridges can be reliably reconstructed, it is simple to ensure.

We introduced fingerprint improvements on the FVC 2004, Biometrika, Italdata, Crossmatch, and Swipe databases to evaluate the performance of the proposed technique. Our technique is compared to other techniques and the technique we propose is superior to enhance fingerprint images. The outcomes of the experiments show that the poor performance fingerprint can be improved exactly with the proposed technique. Experimental findings indicate that the use of the proposed technique allows the extremely accurate fingerprint image to be reconstructed. The average performance of the proposed method is 91.31, which is better than the average performance of another methods. When there exist 18000 features, the running time of UniNap1, ATVS, Dermalog, and CAoS are 68, 74, 59, 87 s respectively, while the running time of the proposed method is 45s. The proposed technique is superior for removing noise than other techniques, in particular for improving fingerprints of poor performance.

For future work, we need to extend the method behavior to deal with spatio-temporal features of fingerprint images to explore the liveness properties. Furthermore, we need to explore the capability of the proposed method in reducing the time complexity of deep learning machine.

References

[1] D. Maltoni, D. Maio, A.K. Jain, and S. Prabhakar, “Handbook of Fingerprint Recognition”, *Springer*, New York, 2003.

[2] W. Wang, J. Li, F. Huang, and H. Feng, “Design and implementation of Log-Gabor filter in fingerprint image enhancement”, *Pattern Recognition Letters*, Vol. 29, No. 3, pp. 301-308, 2008.

[3] Z. Shi, and V. Govindaraju, “A chain code based scheme for fingerprint feature extraction”, *Pattern Recognition Letters*, Vol. 27, No. 5, pp. 462-468, 2006.

[4] D. Das, “A Minutia Detection Approach from Direct Gray-Scale Fingerprint Image Using Hit-or-Miss Transformation”, In: *Proc. of Computational Intelligence in Pattern Recognition*, pp. 195-206, 2020.

[5] M. Patel, S. Parikh, and A. Patel, “An Improved Approach in Fingerprint Recognition Algorithm”, In: *Proc. of Smart Computational Strategies: Theoretical and Practical Aspects*, pp. 135-151, 2019.

[6] H. Fronthaler, K. Kollreider, and J. Bigun, “Local features for enhancement and minutiae extraction in fingerprints”, *IEEE Trans. Image Process*ing, Vol. 17, No. 3, pp. 354-363, 2008.

[7] L. Hong, Y. Wan, and A. K. Jain, “Fingerprint image enhancement: Algorithm and performance evaluation”, *IEEE Trans. Pattern Anal. Mach. Intelligent*, Vol. 20, pp. 777-790, 1998.

[8] L. O’Gorman and J. V. Nickerson, “Matched filter design for fingerprint image enhancement”, In: *Proc. Int. Conf. Acoust. Speech Signal Process*, pp. 916-919, 1998.

[9] J. Yang, L. Liu, T. Jiang, and Y. Fan, “A modified Gabor filter design method for fingerprint image enhancement”, *Pattern Recognition Letters*, Vol. 24, pp. 1805-1817, 2003.

[10] C. Gottschlich, “Curved-region-based ridge frequency estimation and curved Gabor filters for fingerprint image enhancement”, *IEEE Trans. Image Processing*, Vol. 21, pp. 2220-2227, 2012.

[11] C. Gottschlich, “Curved Gabor filters for fingerprint image enhancement”, *Cell and Tissue Research*, Vol. 238, pp. 87-93, 2014.

[12] M. Zahedi, O. Ghadi, “Combining Gabor filter and FFT for fingerprint enhancement based on a regional adaption method and automatic segmentation”, *Signal, Image and Video Processing*, Vol. 9, pp. 267-275, 2015.

[13] J. Bartunek, M. Nilsson, B. Sallberg, and I. Claesson, “Adaptive fingerprint image enhancement with emphasis on preprocessing of data”, *IEEE Transactions on Image Processing*, Vol. 22, No. 2, pp. 644-656, 2012.

[14] P. Sutthiwichaiporn and V. Areekul, “Adaptive boosted spectral filtering for progressive fingerprint enhancement”, *Pattern Recognition*, Vol. 46, pp. 2465-2486, 2013.

[15] M. Khan, T. Khan, D. Bailey, and Y. Kong, “A spatial domain scar removal strategy for

fingerprint image enhancement", *Pattern Recognition*, Vol. 60, pp. 258-274, 2016.
[16] G. Hinton and R. Salakhutdinov, "Reducing the dimensionality of data with neural networks", *Science*, Vol. 313, pp. 504-507, 2006.
[17] G. Hinton and S. Osindero, "A fast learning algorithm for deep belief nets", *Neural Computation*, Vol. 18, pp. 1527-1554, 2006.
[18] R. Salakhutdinov and G. Hinton, "An efficient learning procedure for deep Boltzmann machines", *Neural Computation*, Vol. 24, pp. 1967-2006, 2012.
[19] N. Srivastava, G. Hinton, A. Krizhevsky, I. Sutskever, and R. Salakhutdinov, "Dropout: A Simple Way to Prevent Neural Networks from Overfitting", *Journal of Machine Learning Research*, Vol. 15, pp. 1929-1958, 2014.
[20] Y. LeCun, Y. Bengio, and G. Hinton, "Deep learning", *Nature*, Vol. 521, pp. 436-444, 2015.
[21] S. Kim, B. Park, B. Song, and S. Yang, "Deep belief network based statistical feature learning for fingerprint liveness detection", *Pattern Recognition Letters*, Vol. 77, pp. 58-65, 2016.
[22] M. Kass and A. Witkin, "Analyzing oriented patterns", *Computer Vision, Graphics, and Image Processing*, Vol. 37, No. 3, pp. 362-385, 1987.
[23] A. Bazen and S. Gerez, "Systematic methods for the computation of the directional fields and singular points of fingerprints", *IEEE Trans. Pattern Anal. Mach. Intell*igent, Vol. 24, No. 7, pp. 905-919, 2002.
[24] W. Bian, Y. Luo, D. Xu, and Q. Yu, "Fingerprint ridge orientation field reconstruction using the best quadratic approximation by orthogonal polynomials in two discrete variables", *Pattern Recognition*, Vol. 47, pp. 3304-3313, 2014.
[25] P. Perona, "Orientation diffusions", *IEEE Trans. Image processing*, Vol. 7, No. 3, pp. 457-467, 1998.
[26] J. X, "On orientation and anisotropy estimation for online fingerprint authentication", *IEEE Trans. Signal Processing*, Vol. 53, No. 10, pp. 4038-4049, 2005.
[27] Y. Mei, G. Cao, H. Sun, and R. Hou, "A systematic gradient-based method for the computation of fingerprint's orientation field", *Computers & Electrical Engineering*, Vol. 38, No. 5, pp. 1035-1046, 2012.
[28] W. Bian, S. Ding, and Y. Xue, "Combining weighted linear project analysis with orientation diffusion for fingerprint orientation field reconstruction", *Information Sciences*, Vol. 396, pp. 55-71, 2017.
[29] A. Jain and F. Farrokhnia, "Unsupervised texture segmentation using Gabor filters", *Pattern recognition*, Vol. 24, No. 12, pp. 1167-1186, 1991.
[30] W. Bian, J. Feng, Y. Luo, D. Xu, "The fingerprint enhancement using filtering combined with spectrum diffusion", *Journal of Image and Graphics*, Vol. 19, No. 7, pp. 1021-1030, 2014.
[31] S. Kima, B. Park, B. Song, and S. Yanga, "Deep belief network based statistical feature learning for fingerprint liveness detection", *Pattern Recognition Letters*, Vol. 77, pp. 58–65, 2016.
[32] G. Souza, D. Santos, R. Gonc ¸A. Pires, A. Marana and J. Papa, "Deep features extraction for robust fingerprint spoofing attack detection", *Journal of Artificial Intelligence and Soft Computing Research*, Vol. 9, No. 1, pp. 41-49, 2019.